International Journal of Ambient Energy

ISSN: (Print) (Online) Journal homepage: https://www.tandfonline.com/loi/taen20

# An analytical study of magnetohydrodynamic Casson fluid flow in a channel with induced magnetic field, radiative heat flux and viscous dissipation

Utpal Jyoti Das & Nayan Mani Majumdar

**To cite this article:** Utpal Jyoti Das & Nayan Mani Majumdar (2023): An analytical study of magnetohydrodynamic Casson fluid flow in a channel with induced magnetic field, radiative heat flux and viscous dissipation, International Journal of Ambient Energy, DOI: 10.1080/01430750.2023.2180086

**To link to this article:** https://doi.org/10.1080/01430750.2023.2180086

Published online: 27 Feb 2023.

INTERNATIONAL JOURNAL OF AMBIENT ENERGY
https://doi.org/10.1080/01430750.2023.2180086



# An analytical study of magnetohydrodynamic Casson fluid flow in a channel with induced magnetic field, radiative heat flux and viscous dissipation

Utpal Jyoti Das and Nayan Mani Majumdar

Department of Mathematics, Gauhati University, Guwahati 781014, India

**ABSTRACT**

An analysis of the hydromagnetic flow of an incompressible Casson fluid through a vertical channel with insulated walls is considered. Influences of induced magnetic field, thermal radiation, heat sink, first-order chemical reaction, and viscous dissipation are accounted. The resulting simultaneous coupled equations are solved by using the perturbation technique. The influences of pertinent parameters on fluid velocity, temperature, concentration, induced magnetic field, induced current density, Nusselt number, skin frictions, and mass flux are discussed. It is observed that the Casson parameter and radiation parameter improves the fluid velocity, the Nusselt number, and the skin friction at the two isolated walls. The induced magnetic field in the midline of the channel reduces due to the influences of the chemical reaction parameter and the heat sink parameter, while the Casson parameter increases. The mass flux of the system improves with the Casson parameter, radiation parameter, and chemical reaction parameter.

**ARTICLE HISTORY**
Received 28 October 2022
Accepted 24 January 2023

**KEYWORDS**
Hydromagnetic; Casson fluid; induced magnetic field; thermal radiation; viscous dissipation

## Nomenclature

| | |
|---|---|
| $Bi$ | Biot number |
| $Ci$ | Solutal Biot number |
| $C_0^*, C_d^*$ | concentration of vertical walls (Mol/m$^3$) |
| $C^*$ | concentration of the fluid in dimensional form (Mol/m$^3$) |
| $C$ | concentration in non-dimensional form |
| $C_p$ | heat capacity at constant pressure (J/(K.kg)) |
| $d$ | distance between the two walls (m) |
| $D$ | mass diffusivity (m$^2$/s) |
| $Ec$ | Eckert number |
| $G$ | Grashof number |
| $G_1$ | Solutal Grashof number |
| $g$ | acceleration due to gravity (m/s$^2$) |
| $h^*$ | induced magnetic field at $z^*$- direction (A/m) |
| $Ha$ | Hartmann number |
| $H_0^*$ | magnetic field (A/m) |
| $I$ | non-dimensional IMF |
| $Kr$ | chemical reaction parameter ($s^{-1}$) |
| $Q_o$ | heat generation/absorption coefficient (W/(m$^2$.K)) |
| $q_r$ | radiative heat flux (W/m$^2$) |
| $Rd$ | radiation parameter |
| $S$ | heat source/sink parameter |
| $Sc$ | Schmidt number |
| $T_0^*, T_d^*$ | temperature of vertical walls (K) |
| $T^*$ | temperature of the fluid (K) |
| $T$ | non-dimensional temperature |
| $U$ | characteristic- velocity (m/s) |
| $u^*$ | velocity in $x^*-$direction (m/s) |
| $W$ | non-dimensional velocity |

### *Greek Symbols*

| | |
|---|---|
| $\beta'$ | coefficient of thermal expansion (1/K) |
| $\beta_c$ | coefficient of mass expansion (m$^3$/Mol) |
| $\epsilon$ | electrical permittivity (F/m) |
| $\kappa$ | thermal conductivity (W/(m.K)) |
| $\mu$ | coefficient of viscosity (kg/(m.s)) |
| $\nu$ | kinematic viscosity of the fluid (m$^2$/s) |
| $\lambda$ | non-dimensional chemical reaction parameter |
| $\mu_e$ | magnetic permeability (H/m) |
| $\sigma$ | electrical conductivity (A$^2$S$^{-3}$/(kg.m$^2$)) |
| $\rho$ | fluid density (kg/m$^3$) |
| $\tau_0, \tau_1$ | skin-friction |
| $\sigma^*$ | Stefan–Boltzmann constant |
| $\delta^*$ | mean absorption coefficient |

## 1. Introduction

Casson is referred to as a shear-thinning liquid that is understood to have non-finite viscosity at zero-rated of shear. Casson fluid has a very important role in the fields like medical, chemicals, biologicals, and engineering. Also, Casson fluid is used in drilling operations and food processing. Casson devised the Casson fluid model in 1959 for predicting flow patterns of suspended pigment oil (Casson 1959). Honey, jelly, soup, concentrated fruit liquids, and artificial fibres are all examples of Casson fluid. Casson fluid may be found in the manufacturing of a wide range of substances, including synthetic lubricants, medicinal compounds, paints, coal, tomato sauce, China clay, and several others. As human blood contains numerous elements such

**CONTACT** Nayan Mani Majumdar nayanm.majumdar@gmail.com

as fibrinogen, human red blood cells, protein, and globulin in aqueous base plasma, it is also known as Casson fluid. Casson fluid's effective uses in drilling processes, biological treatments, food processing, and bio-engineering activities have captured the attention of a wide range of researchers. Many investigators investigated some research on Casson fluids such as Mukhopadhyay et al. (2013), Pramanik (2014), Arthur, Seini, and Bortteir (2015) studied in the presence of the magnetic field, the flow of Casson fluid over a porous surface with some chemical reaction. In 2018, Krishna, Reddy, and Makinde (2018) investigated the effect of chemical reaction with a porous stretching sheet of Casson fluid on MHD flow. Mohamad et al. (2019) studied the impact of rotating a Casson fluid on an operating channel disk. In the industrial environment, many scholars executed their research work on the effects of various parameters on the Casson fluid. Recently, Abdullahi, Wala, and Sani (2020), Anandha Kumar et al. (2022), Asogwa and Ibe (2020), Das (2021), Ramudu et al. (2021), Sandeep, Sulochana, and Ashwinkumar (2022), Reddy et al. (2022), Hussain, Zeeshan, and Sagheer (2022), Saranya, Al-Mdallal, and Animasaun (2022), Vishnu Ganesh et al. (2022a), Vishnu Ganesh et al. (2022b), etc investigated the characteristics of Casson fluid flow.

The study of the dynamics of electrically conducting fluids in the presence of a magnetic field is called magnetohydrodynamics (MHD). Cramer (1973) presented a summary of magnetohydrodynamic flow as well as the induced magnetic field in industrial and engineering applications. Many researchers such as Jha and Apere (2011), Hamza, Usman, and Sule (2015), and Sheikholeslami et al. (2016) have presented hydromagnetic flow with various geometries and methods. Gregory et al. (2016) and Rashidi, Esfahani, and Maskaniyan (2017) presented the MHD flow and its mathematical modelling in biological systems. Krishna, Jyothi, and Chamkha (2020) investigated the MHD flow of second-grade fluid through a porous medium over a semi-infinite vertical stretching sheet. Recently, Sharma, Choudhury, and Das (2022), Nayak, Acharya, and Mishra (2022), Hussain, Aly, and Öztop (2022), and Hussain et al. (2022) investigated the MHD flow.

In investigations of hydromagnetic convective flows, the effect of the induced magnetic field has been neglected in many studies to facilitate the mathematical analysis of such a simple problem. The induced magnetic field also generates its own magnetic field in the fluid and consequently the original magnetic field changes; at the same time, the flux in the magnetic field produces mechanical forces that modify the movement of the fluid. Therefore, in many situations, it is necessary to include the effect of the induced magnetic field in the hydromagnetic equations. Many researchers have considered the effect of the induced magnetic field in their studies, such as Globe (1959), Arora (1972), Guria et al. (2007), and Singh et al. (2010), who have considered that effects in their magnetohydrodynamic flow analysis. In addition, Singh and Singh (2012) analysed the importance of the induced magnetic field, such as an electric field passage in upward concentric cylinders. Jha and Isa (2013) explained the effect of an induced magnetic field on the electric flow of non-artificial convection between the vertical channel and also considered the heating effect identically. Also, the effect of induced magnetic field is considered by Sarveshanand and Singh (2015) in their research work. Jha and Aina (2017) investigated the effect of an induced magnetic field for MHD flow with non-artificial convection using a micro-channel with parallelly vertical electric walls at the same distance. Kumar, Singh, and Kumar (2020) investigated the effect of induced magnetic field on the convective flow between vertical parallel plates with the Hall effect. Kumar (2021) studied the impact of Newtonian cooling/heating with an induced magnetic field in a channel for a Newtonian fluid. Shah et al. (2022) studied the impact of an induced magnetic field on magnetohydrodynamic convective flow in a rectangular channel of two immiscible fluids.

Recently, Hussain, Aly, and Alsedias (2022), Hussain, Alsedias, and Aly (2022), Gokulavani, Muthtamilselvan, and Al-Mdallal (2022) studied heat and mass transfer flows with different geometries. Thermal radiation is mainly electromagnetic radiation which is generated by the thermal motion of all particles in matter. Thermal radiation is the outflow of electromagnetic waves that from all the particles which have temperatures very large than absolute zero. Many researches have been done by researchers. Some of them are Shateyi and Motsa (2009), Elbashbeshy and Emam (2011). Kho et al. (2017), Daniel et al. (2018), Sedki et al. (2021), Kumar et al. (2021), Prakash et al. (2021), Hussain, Raizah, and Aly (2022), etc.

Viscous dissipation is very important in the flow of fluids having high velocities, which increases the temperature of the fluid. Generally, viscous dissipation is defined as the transformation of kinetic energy to internal energy (heating up the fluid) due to viscosity which includes both turbulent kinetic energy and mean flow kinetic energy. In 1951, Brinkman (1951), initiated research on the viscous dissipation. Basu and Roy (1985) studied the effect of viscous dissipation on the laminar flow problem in a tube. Jha and Aina (2018) studied the effect of viscous dissipation on completely progressed natural convection flow in a vertical microchannel. Recently, Vijayalakshmi and Govindarajan (2019), Naseem et al. (2022), Loh, Chen, and Lim (2022), and Hassan et al. (2022) presented the impact of viscous dissipation.

Here, our objective is to study the Casson fluid flow with an induced magnetic field in a vertical channel, incorporating the influences of viscous dissipation, heat source/sink, first-order chemical reaction, and thermal radiation. This study is an extension of the study of Kumar (2021) on Casson fluids by incorporating heat source/sink parameter, viscous dissipation, and first-order chemical reaction.

## 2. Mathematical analysis

Consider a fully developed, incompressible, viscous, steady, chemically reacting hydromagnetic flow of Casson fluid through a vertical channel having insulated walls.

The x-axis is taken along the vertical parallel-insulated walls and the y and z-axes are taken as shown in Figure 1. Here, the influences of the induced magnetic field (IMF), radiative heat flux, first-order chemical reaction, viscous dissipation, and heat sink are considered.

Then, the governing equations following Sarveshanand and Singh (2015), and Kumar (2021) become:

$$\nu\left(1+\frac{1}{\beta}\right)\frac{d^2u^*}{dz^{*2}}+\frac{\mu_e H_0^*}{\rho}\frac{dh^*}{dz^*}+g\beta'(T^*-T_d^*)+g\beta_c(C^*-C_d^*)=0 \tag{1}$$

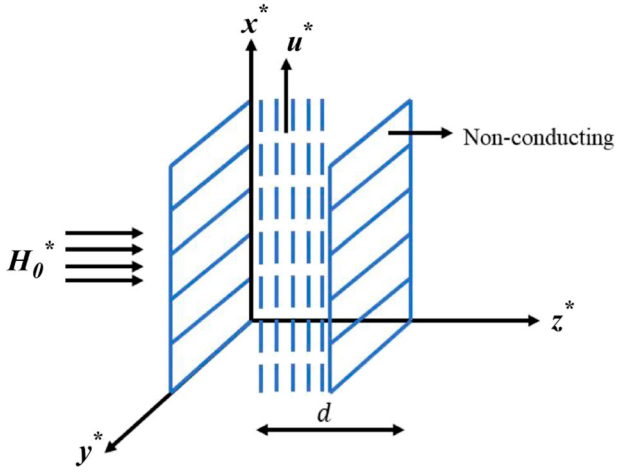


**Figure 1.** Geometrical shape for considered model.

$$\frac{d^2h^*}{dz^{*2}} + \sigma\mu_e H_0^* \frac{du^*}{dz^*} = 0 \tag{2}$$

$$\frac{\kappa}{\rho C_p}\frac{d^2T^*}{dz^{*2}} - \frac{Q_0}{\rho C_p}(T^* - T_d^*) - \frac{1}{\rho C_p}\frac{dq_r}{dz^*} + \frac{\nu}{C_p}\left(1+\frac{1}{\beta}\right)\left(\frac{du}{dz^*}\right)^2 + \frac{1}{\sigma\rho C_p}\left(\frac{dh^*}{dz^*}\right)^2 = 0 \tag{3}$$

$$D\frac{d^2C^*}{dz^{*2}} - Kr(C^* - C_d{}^*) = 0 \tag{4}$$

where $\beta$ is the Casson parameter and other symbols are mentioned in the nomenclature section.

The boundary restrictions are (Kumar [2021]):

$$\begin{aligned} &u^* = 0,\ h^* = 0,\ \frac{dT^*}{dz^*} = \alpha_1(T^* - T_d^*), \\ &\frac{dC^*}{dz^*} = \alpha_2(C^* - C_d^*) \quad \text{at } z^* = 0, \\ &u^* = 0,\ h^* = 0,\ T^* = T_0^*,\ C^* = C_0^* \quad \text{at } z^* = d, \end{aligned} \tag{5}$$

Using Rosseland approximation, we take the $q_r$ (radiative heat flux) as:

$$q_r = -\frac{4\sigma^*}{3\delta^*}\frac{\partial T^{*4}}{\partial z^*} \tag{6}$$

Here, also, we write $T^{*4}$ in the Taylor series around $T_0^*$, where $T_0^*$ is the free stream temperature and omitting higher order terms, we get

$$T^{*4} \equiv T_0^{*3}(4T^* - 3T_0^*) \tag{7}$$

Using Equations (6) and (7) into Equation (3), we get

$$\frac{\kappa}{\rho C_p}\frac{d^2T^*}{dz^{*2}} - \frac{Q_0}{\rho C_p}(T^* - T_d^*) + \frac{16\sigma^* T_0^{*3}}{3\delta^*\rho C_p}\frac{d^2T^*}{dz^{*2}} + \nu\left(1+\frac{1}{\beta}\right)\left(\frac{du}{dz^*}\right)^2 + \frac{1}{\sigma Q C_p}\left(\frac{dh^*}{dz^*}\right)^2 = 0 \tag{8}$$

Acknowledging similarity transformations

$$\begin{aligned} &W = \frac{u^*}{U},\ z = \frac{z^*}{d},\ I = \frac{h^*}{\sigma\mu_e H_0^* U d},\ T = \frac{T^* - T_d^*}{T_0^* - T_d^*}, \\ &C = \frac{C^* - C_d^*}{C_0^* - C_d^*},\ Ha = \mu_e H_0^* d\sqrt{\frac{\sigma}{\mu}}, \\ &Ec = \frac{U^2}{C_p(T_0^* - T_d^*)},\ G = \frac{g\beta' d^2(T_0^* - T_d^*)}{U\nu}, \\ &G_1 = \frac{g\beta_c d^2(C_0^* - C_d^*)}{U\nu},\ S = \frac{Q_0 d^2}{\kappa}, \\ &Rd = \frac{16\sigma^* T_0^{*3}}{3\kappa\delta^*}, Bi = \alpha_1 d,\ Ci = \alpha_2 d,\ Sc = \frac{\nu}{D},\ \lambda = \frac{Kr\, d^2}{\nu} \end{aligned} \tag{9}$$

The Equations (1), (2), (8), (4) reduce to

$$\left(1+\frac{1}{\beta}\right)\frac{d^2W}{dz^2} + Ha^2\frac{dI}{dz} + GT + G_1C = 0 \tag{10}$$

$$\frac{d^2I}{dz^2} + \frac{dW}{dz} = 0 \tag{11}$$

$$(1+Rd)\frac{d^2T}{dz^2} - ST + EcPr\left(1+\frac{1}{\beta}\right)\left(\frac{dW}{dz}\right)^2 + Ha^2PrEc\left(\frac{dI}{dz}\right)^2 = 0 \tag{12}$$

$$\frac{d^2C}{dz^2} - \lambda ScC = 0 \tag{13}$$

with restrictions

$$\begin{aligned} &W = 0,\ I = 0,\ \frac{dC}{dz} = CiC,\ \frac{dT}{dz} = BiT \quad \text{at } z = 0 \\ &W = 0,\ I = 0,\ C = 1,\ T = 1 \quad \text{at } z = 1 \end{aligned} \tag{14}$$

## 3. Method of the solution

The solution of Equation (13) under the boundary conditions (14) is

$$C = A_1e^{m_1z} + A_2e^{-m_1z} \tag{15}$$

The paired differential Equations (10)–(12) with relevant restrictions (14) can be solved by using the perturbation technique. As Eckert number ($Ec << 1$) is very small, so, for solutions of Equations (11)–(13), we introduce

$$\begin{aligned} W(z) &= W_0(z) + EcW_1(z) + o(Ec^2) \\ I(z) &= I_0(z) + EcI_1(z) + o(Ec^2) \\ T(z) &= T_0(z) + EcT_1(z) + o(Ec^2) \end{aligned} \tag{16}$$

Using Equation (16), Equations (10–12) reduces to the following form

**Zeroth order equations:**

$$BW_0'' + Ha^2I_0' + GT_0 + G_1C = 0 \tag{17}$$

$$I_0'' + W_0' = 0 \tag{18}$$

$$(1+Rd)T_0'' - ST_0 = 0 \tag{19}$$

**First-order equations:**

$$BW_1'' + Ha^2I_1' + GT_1 = 0 \tag{20}$$

$$I_1'' + W_1' = 0 \tag{21}$$

$$(1 + Rd)T_1'' - ST_1 + PrBW_0'^2 + Ha^2 PrI_0'^2 = 0 \tag{22}$$

With the boundary restrictions

$$\begin{aligned} &W_0 = 0,\ W_1 = 0,\ I_0 = 0,\ I_1 = 0,\ T_0' = BiT_0, \\ &T_1' = BiT_1 \quad \text{at } z = 0 \\ &W_0 = 0,\ W_1 = 0,\ I_0 = 0,\ I_1 = 1,\ T_0 = 1, \\ &T_1 = 0 \quad \text{at } z = 0 \end{aligned} \tag{23}$$

Solving the Equations (17)–(22) under restrictions (23), we get

$$T_0 = A_3 e^{Nz} + A_4 e^{-Nz} \tag{24}$$

$$\begin{aligned} I_0 = {} & A_5 + A_6 e^{Kz} + A_7 e^{-Kz} + A_{10} e^{Nz} - A_{11} e^{-Nz} \\ & + A_{12} e^{m_1 z} - A_{13} e^{-m_1 z} \end{aligned} \tag{25}$$

$$\begin{aligned} W_0 = {} & A_{14} - A_6 K e^{Kz} + A_7 K e^{-Kz} - A_{10} N e^{Nz} - A_{11} N e^{-Nz} \\ & - A_{12} m_1 e^{m_1 z} - A_{13} m_1 e^{-m_1 z} \end{aligned} \tag{26}$$

$$\tau_1 = -\left(\frac{dW}{dz}\right)_{z=1} = -\left[\left(\frac{dW_0}{dz}\right) + Ec\left(\frac{dW_1}{dz}\right)\right]_{z=1} \tag{32}$$

The mass flux($Q$) is obtained as

$$Q = \frac{Q^*}{Ud} = \int_{z=0}^{z=1} W(z)dz, \text{ where } Q^* = \int_{z^*=0}^{z^*=d} u^* dz^* \tag{33}$$

The Nusselt number at the surfaces $z = 0$ and $z = 1$ are

$$Nu]_{z=0,1} = \frac{dq_W}{\kappa(T_0{}^* - T_d{}^*)}, \quad \text{where } q_W = -\left(\kappa \frac{\partial T^*}{\partial z^*}\right)_{z^*=0,d}$$

Thus,

$$Nu_0 = -\left(\frac{dT}{dz}\right)_{z=0} = -\left[\left(\frac{dT_0}{dz}\right) + Ec\left(\frac{dT_1}{dz}\right)\right]_{z=0} \tag{34}$$

$$Nu_1 = -\left(\frac{dT}{dz}\right)_{z=1} = -\left[\left(\frac{dT_0}{dz}\right) + Ec\left(\frac{dT_1}{dz}\right)\right]_{z=1} \tag{35}$$

$$T_1 = \begin{bmatrix} A_{15}e^{Nz} + A_{16}e^{-Nz} + A_{74}e^{2Kz} + A_{75}e^{-2Kz} + A_{76}e^{2Nz} + A_{77}e^{-2Nz} + A_{78}e^{2m_1 z} + \\ A_{79}e^{-2m_1 z} + A_{80} + A_{81}e^{(K+N)z} + A_{82}e^{-(K+N)z} + A_{83}e^{(K-N)z} + A_{84}e^{-(K-N)z} + \\ A_{85}e^{(K+m_1)z} + A_{86}e^{-(K+m_1)z} + A_{87}e^{(K-m_1)z} + A_{88}e^{-(K-m_1)z} + A_{89}e^{(N+m_1)z} + \\ A_{90}e^{-(N+m_1)z} + A_{91}e^{(N-m_1)z} + A_{92}e^{-(N-m_1)z} \end{bmatrix} \tag{27}$$

$$I_1 = \begin{bmatrix} A_{93} + A_{94}e^{Kz} + A_{95}e^{-Kz} + A_{96}e^{Nz} - A_{97}e^{-Nz} + A_{98}e^{2Kz} - A_{99}e^{-2Kz} + A_{100}e^{2Nz} - \\ A_{101}e^{-2Nz} + A_{102}e^{2m_1 z} - A_{103}e^{-2m_1 z} + A_{104}z + A_{105}e^{(K+N)z} - A_{106}e^{-(K+N)z} + \\ A_{107}e^{(K-N)z} - A_{108}e^{-(K-N)z} + A_{109}e^{(K+m_1)z} - A_{110}e^{-(K+m_1)z} + A_{111}e^{(K-m_1)z} - \\ A_{112}e^{-(K-m_1)z} + A_{113}e^{(N+m_1)z} - A_{114}e^{-(N+m_1)z} + A_{115}e^{(N-m_1)z} - A_{116}e^{-(N-m_1)z} \end{bmatrix} \tag{28}$$

$$W_1 = \begin{bmatrix} A_{117} - A_{94}Ke^{Kz} + A_{95}Ke^{-Kz} - A_{96}Ne^{Nz} - A_{97}Ne^{-Nz} - 2A_{98}Ke^{2Kz} - 2A_{99}Ke^{-2Kz} \\ -2A_{100}Ne^{2Nz} - 2A_{101}Ne^{-2Nz} - 2A_{102}m_1 e^{2m_1 z} - 2A_{103}m_1 e^{-2m_1 z} - A_{104} - \\ (K+N)A_{105}e^{(K+N)z} - (K+N)A_{106}e^{-(K+N)z} - (K-N)A_{107}e^{(K-N)z} - \\ (K-N)A_{108}e^{-(K-N)z} - (K+m_1)A_{109}e^{(K+m_1)z} - (K+m_1)A_{110}e^{-(K+m_1)z} - \\ (K-m_1)A_{111}e^{(K-m_1)z} - (K-m_1)A_{112}e^{-(K-m_1)z} - (N+m_1)A_{113}e^{(N+m_1)z} - \\ (N+m_1)A_{114}e^{-(N+m_1)z} - (N-m_1)A_{115}e^{(N-m_1)z}(N-m_1)A_{116}e^{-(N-m_1)z} \end{bmatrix} \tag{29}$$

The induced current density is:

$$\begin{aligned} J(z) &= -\left(\frac{dI}{dz}\right) \\ &= \begin{bmatrix} -A_6Ke^{Kz} + A_7Ke^{-Kz} - A_{10}Ne^{Nz} - A_{11}Ne^{-Nz} - A_{12}m_1e^{m_1z} - A_{13}m_1e^{-m_1z} - \\ A_{94}Ke^{Kz} + A_{95}Ke^{-Kz} - A_{96}Ne^{Nz} - A_{97}Ne^{-Nz} - 2A_{98}Ke^{2Kz} - 2A_{99}Ke^{-2Kz} - \\ 2A_{100}Ne^{2Nz} - 2A_{101}Ne^{-2Nz} - 2A_{102}m_1e^{2m_1z} - 2A_{103}m_1e^{-2m_1z} - A_{104} - \\ (K+N)A_{105}e^{(K+N)z} - (K+N)A_{106}e^{-(K+N)z} - (K-N)A_{107}e^{(K-N)z} - \\ (K-N)A_{108}e^{-(K-N)z} - (K+m_1)A_{109}e^{(K+m_1)z} - (K+m_1)A_{110}e^{-(K+m_1)z} - \\ (K-m_1)A_{111}e^{(K-m_1)z} - (K-m_1)A_{112}e^{-(K-m_1)z} - (N+m_1)A_{113}e^{(N+m_1)z} - \\ (N+m_1)A_{114}e^{-(N+m_1)z} - (N-m_1)A_{115}e^{(N-m_1)z} - (N-m_1)A_{116}e^{-(N-m_1)z} \end{bmatrix} \end{aligned} \tag{30}$$

The skin frictions at the surfaces $z = 0$ and $z = 1$ are:

$$\tau]_{z=0,1} = \frac{\tau_W}{\left(\frac{\mu U}{d}\right)}, \text{ where } \tau_W = \left(\mu \frac{\partial u^*}{\partial z^*}\right)_{z^*=0,d}$$

Thus,

$$\tau_0 = +\left(\frac{dW}{dz}\right)_{z=0} = +\left[\left(\frac{dW_0}{dz}\right) + Ec\left(\frac{dW_1}{dz}\right)\right]_{z=0} \tag{31}$$

## 4. Results and discussion

In this section, the impacts of various parameters that affect the characteristics of flow, heat, and mass transfer have been graphically represented.

The following values are assigned to the parameters:

$$Sc = 0.9\,; Ha = 5\,; S = 1\,; G = 1\,; G_1 = 1\,; Bi = 0.7\,; Pr = 0.63\,;$$

$\beta = 2; Rd = 1; \gamma = 1$

Figures 2–6 represent the velocity profile for the Casson parameter ($\beta$), chemical reaction parameter ($\gamma$), radiation parameter($Rd$), heat sink parameter ($S$), Schmidt number ($Sc$), respectively.

It is found that the velocity profiles are nearly parabolic in nature having the maximum value near the centreline of the channel.

Figure 2 shows that the rising Casson parameter from $\beta = 1$ to $\beta = 4$ through $\beta = 2$ raises the fluid velocity. It is significant to note that the fluid reduces to Newtonian when $\beta \to \infty$. Therefore, compared to Casson fluid, Newtonian fluid has a thicker momentum boundary layer.

Figure 3 shows that the fluid velocity reduced with the rise in the chemical reaction parameter. Thus, the fluid motion is slowed due to the chemical reaction, indicating that the consumption of chemical species causes a reduction in the

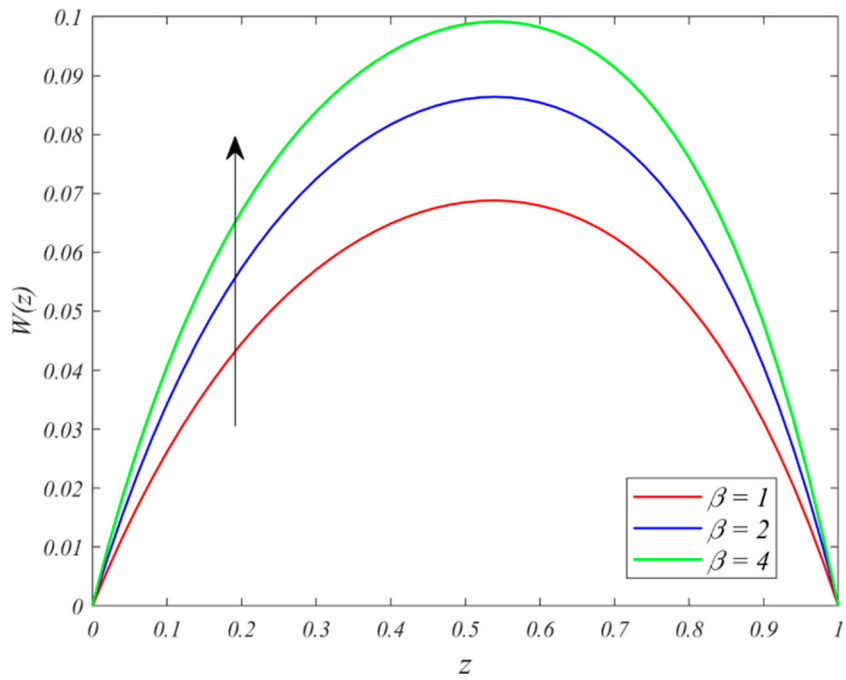


**Figure 2.** Effect of $\beta$ in W.

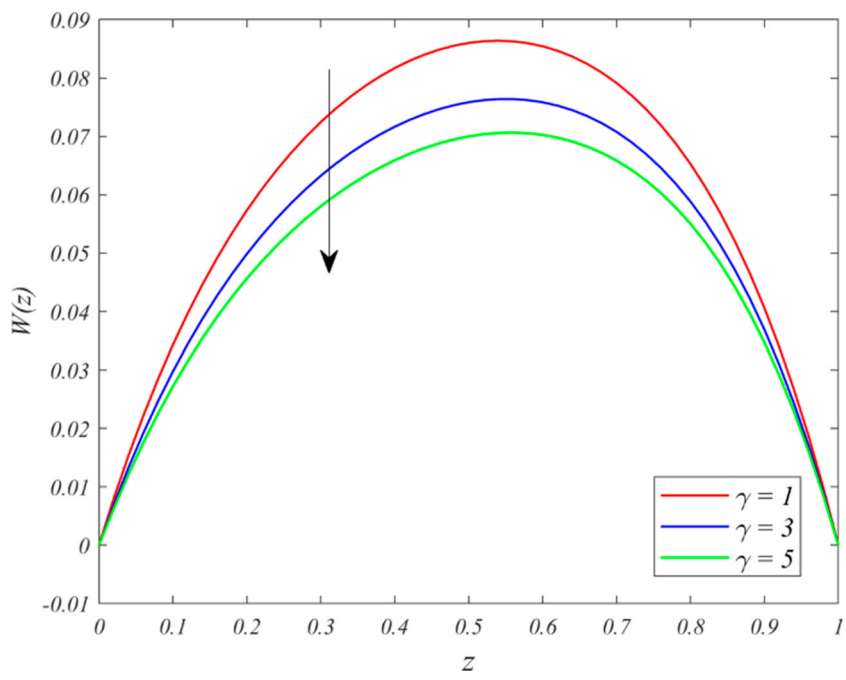


**Figure 3.** Effect of $\gamma$ in W.

concentration field, which lowers the buoyant effects caused by concentration gradients. As a result, the fluid flow retarded.

Figure 4 shows that the *Rd* produces a significant rise in the fluid velocity. Physically, the increase in the thermal radiation parameter causes a considerable increase in the thermal conditions in the temperature of the fluid, which determines more fluid in the boundary layer due to the buoyancy effect and therefore increases the velocity in the fluid. This result agrees well with Kumar (2021).

Figure 5 shows that increasing values of $S$ from $S = -1$ (heat source) to $S = 3$ (heat sink) through $S = 1$ (heat sink) reduce the width of the momentum boundary layer. This is because, when heat is absorbed, there is a decrease in the buoyancy force and the flow field is affected by negative effects and leads to a depreciation of the speed values.

From Figure 6, it is observed that an intensification in the Schmidt number ($Sc$) leads to a lessening in the fluid velocity due to a decrease in molecular diffusivity, which leads to a reduction in the fluid velocity.

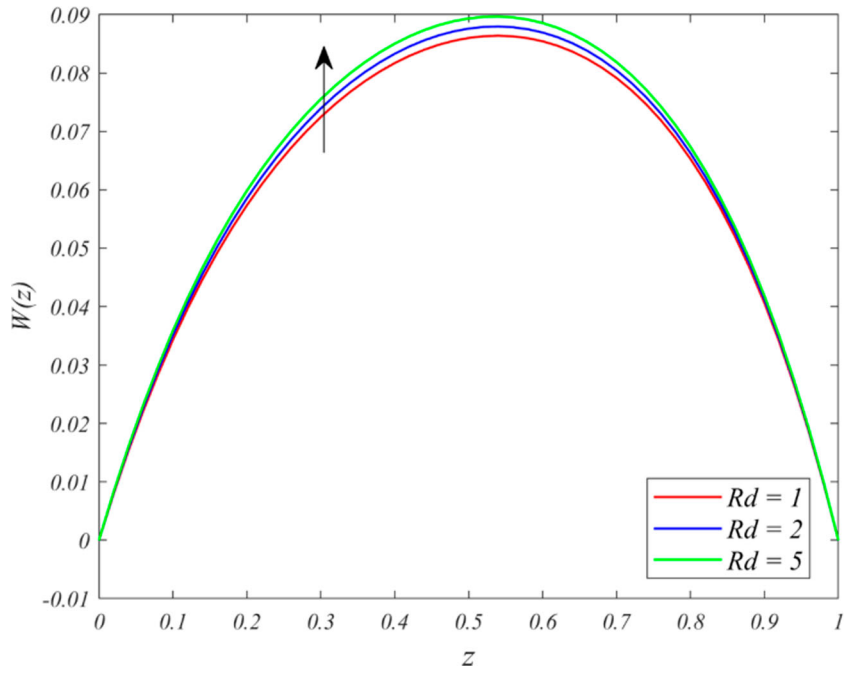


**Figure 4.** Effect of Rd in W.

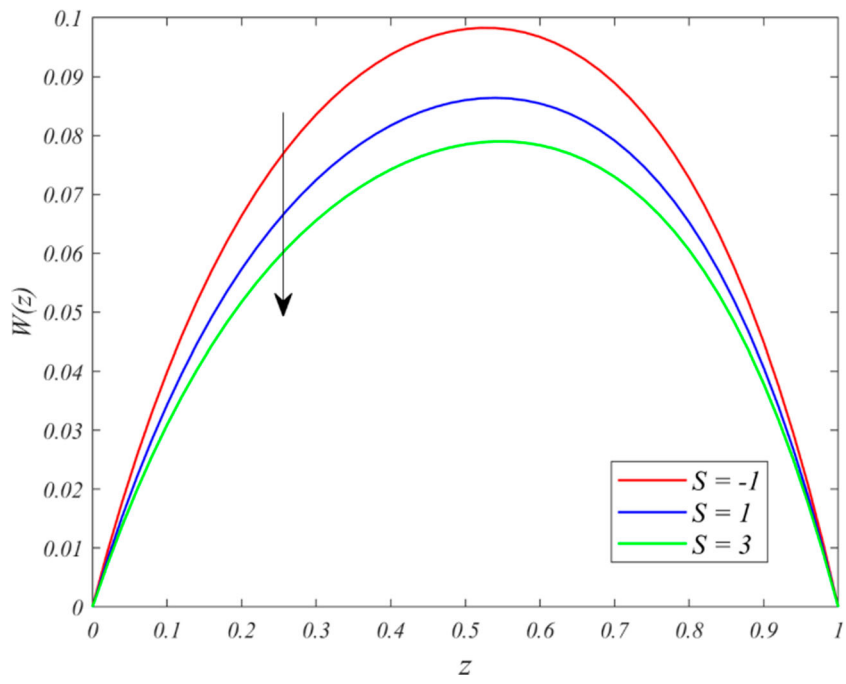


**Figure 5.** Effect of S in W.

Figures 7–9 represent the plots of induced magnetic field (IMF) for various Casson parameter, thermal Grashof number, and chemical reaction parameter, respectively.

It is observed that the values of IMF rise with the increase in the values of $\beta$ and $G$ when $z \in (0,\ 0.54)$, while it shows a reverse trend when $z \in (0.54,\ 1)$.

Figure 9 shows that the IMF declines with the increase in chemical reaction parameter when $z \in (0,\ 0.5)$, while it shows an opposite trend when $z \in (0.5,\ 1)$.

Figures 10–12 represent the plots of ICD for various Casson parameter, Eckert number, and chemical reaction parameter, respectively.

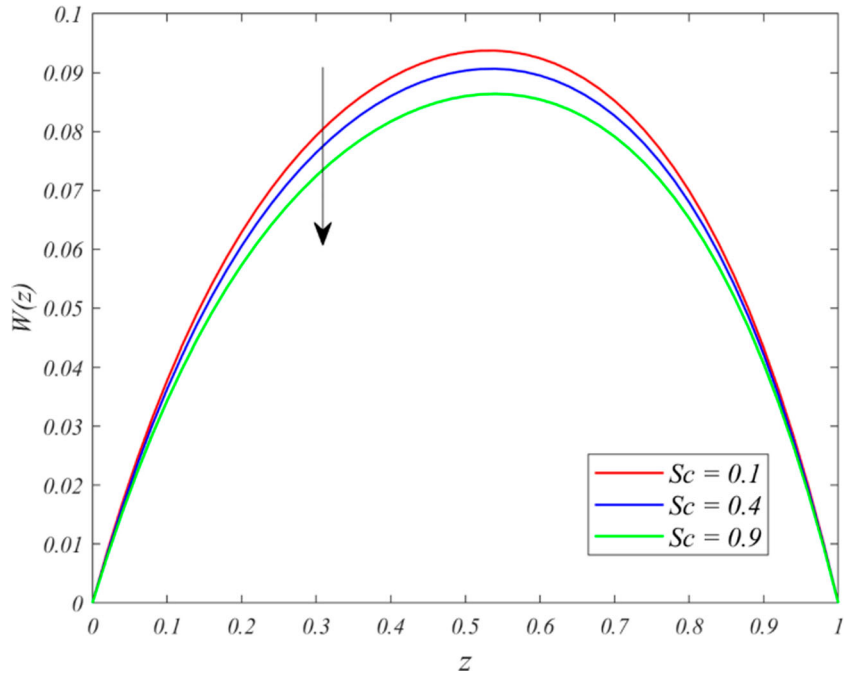


**Figure 6.** Effect of Sc in W.

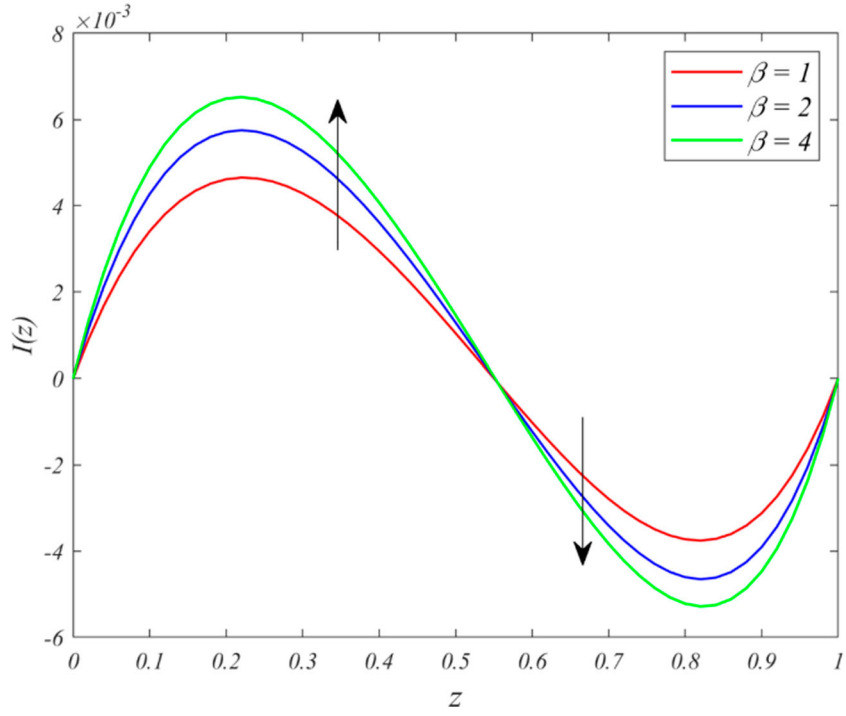


**Figure 7.** Effect of $\beta$ in I.

Figure 10 shows that by increasing the Casson parameter, the ICD of fluid decreases significantly when $z \in (0,\ 0.2)$ and when $z \in (0.85,\ 1)$, but a reverse trend is seen when $z \in (0.20.85)$.

Figure 11 shows that by raising S from $S = -1$ (heat source) to $S = 3$ (heat sink) through $S = 1$ (heat sink), the ICD of fluid improved when $z \in (0,\ 0.2)$ and$(0.8,\ 1)$, while the opposite behaviour is seen when $z \in (0.2,\ 0.8)$.

Figure 12 shows that the ICD of the fluid amplifies with the effect of the chemical reaction parameter when $z \in (0,\ 0.2)$ and $(0.8,\ 1)$, but declines when $z \in (0.2,\ 0.8)$.

Figures 13–15 represent the plots of temperature profile for various $S$, $Bi$, and $Ec$, respectively.

Figure 13 shows that the temperature profile of fluid reduces for increasing $S$. This is due to the effect that added heat

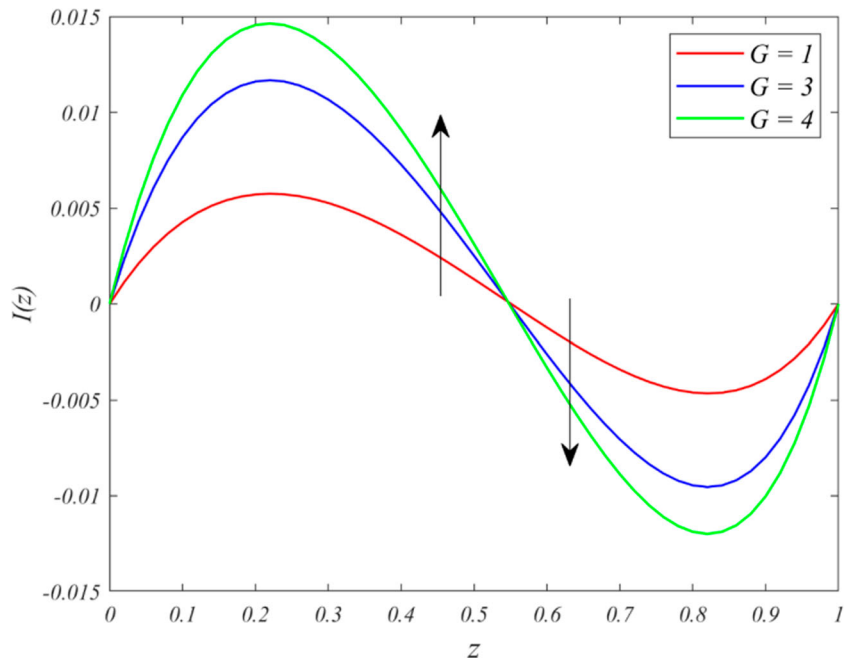


**Figure 8.** Effect of G in I.

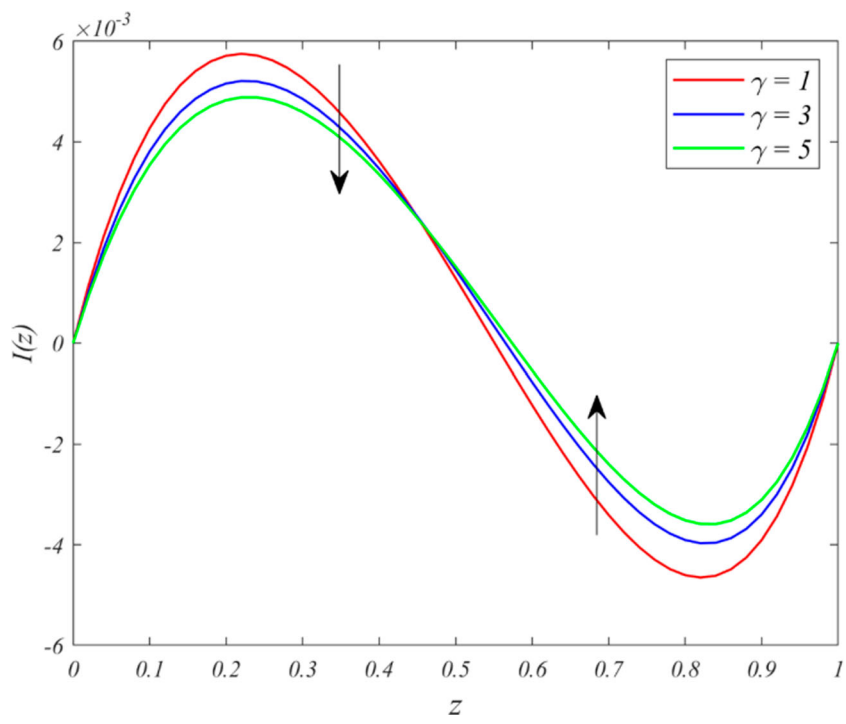


**Figure 9.** Effect of $\gamma$ in I.

sink causes a reduction in thermal energy as well as kinetic energy, and consequently reduces the thickness of the thermal boundary layer. A similar effect is seen for *Bi* as observed in Figure 14.

Figure 15 shows that the rise in *Ec* raises the fluid temperature. Physically, increasing Eckert number increases the kinetic energy of the fluid inside the thermal boundary layer and thus increases the temperature of the fluid.

Figures 16–18 represent the plots of the concentration profile for various *Bi*, $\gamma$, and *Sc*, respectively.

It shows that the amplification in *Bi* (Figure 16), $\gamma$ (Figure 17), and *Sc* (Figure 18) reduces the fluid concentration. Increasing the chemical reaction parameter results in an increase in the number of solute molecules performing chemical reactions, which causes the concentration field to drop. A rise in Schmidt number decreases mass diffusivity so concentration decreases.

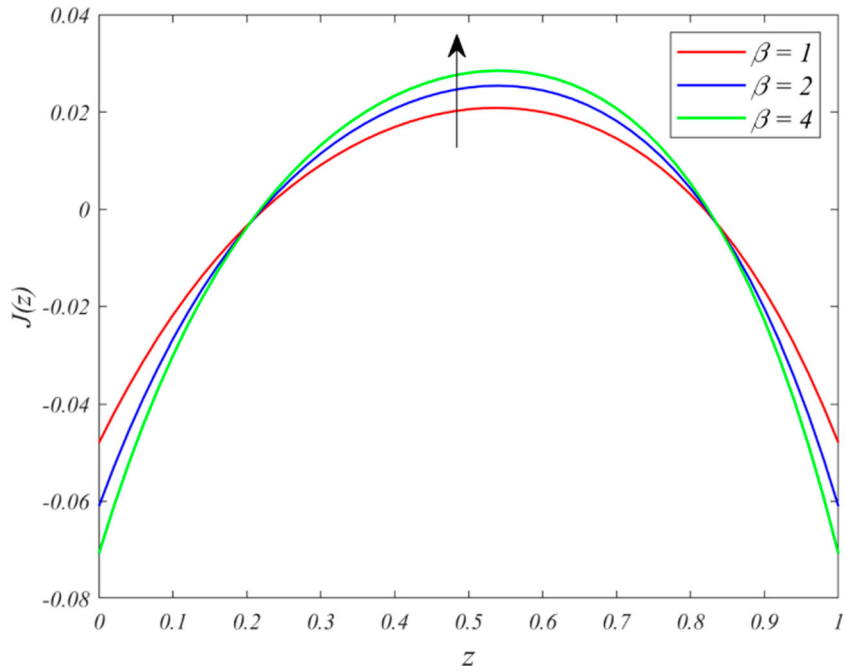


**Figure 10.** Effect of $\beta$ in J.

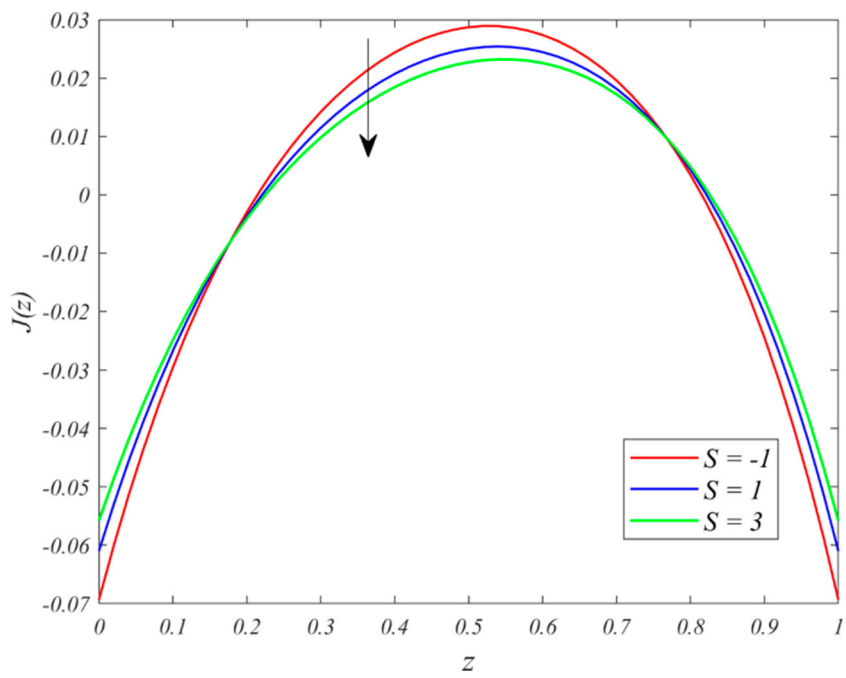


**Figure 11.** Effect of S in J.

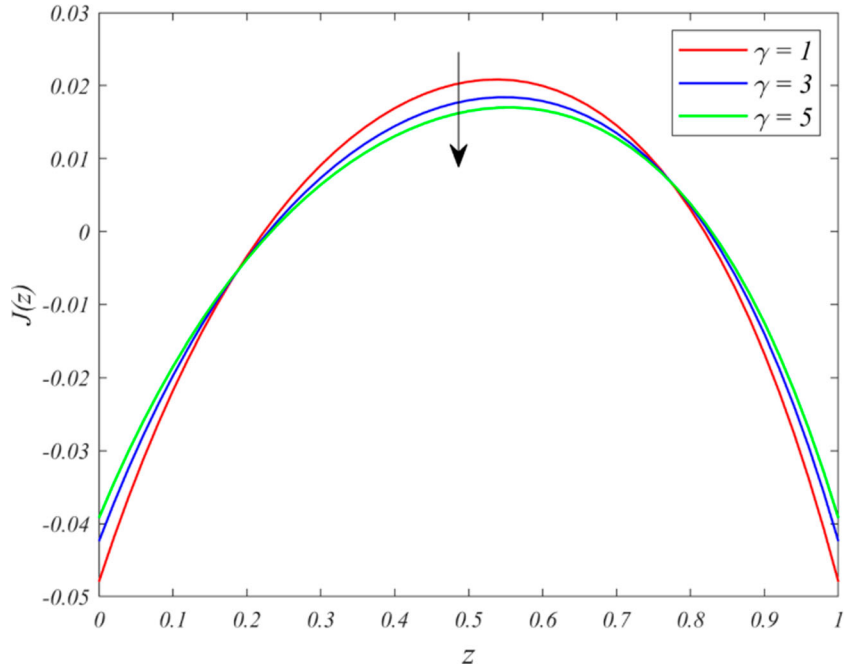


**Figure 12.** Effect of $\gamma$ in J.

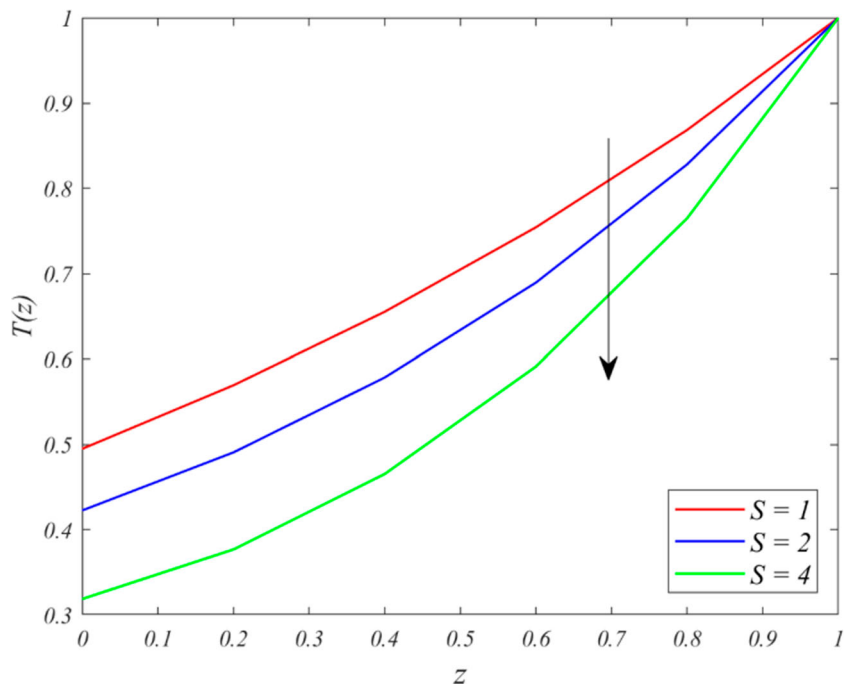


**Figure 13.** Effect of S in T.

Table 1 shows the calculated values of the Nusselt number $Nu_0$ and $Nu_1$ at the surfaces $z = 0$ and $z = 1$, respectively. It is seen that $\beta$, $Rd$, and $Ec$ amplify the $Nu_0$ and $Nu_1$.

Table 2 shows the calculated values of skin friction and mass flux. It shows that $\beta$, $Rd$, and $Ec$ amplify the skin friction values $\tau_0$ and $\tau_1$ at the surfaces $z = 0$ and $z = 1$, respectively, whereas an opposite trend is observed for the chemical reaction parameter $\gamma$. Furthermore, the mass flux is seen to rise due to the intensification in $\beta$, $Rd$, and $Ec$, whereas $\gamma$ shows opposite trend.

## 5. Validity and comparison

The novelty of this study lies in the investigation of the effects of viscous dissipation, heat source/sink parameter, and first-order chemical reaction in the MHD Casson fluid flow in a channel.

In the absence of a chemical reaction, the present study is well validated through the study of Kumar (2021), when $\beta \to \infty$, $S = 0$ and $Ec = 0$.

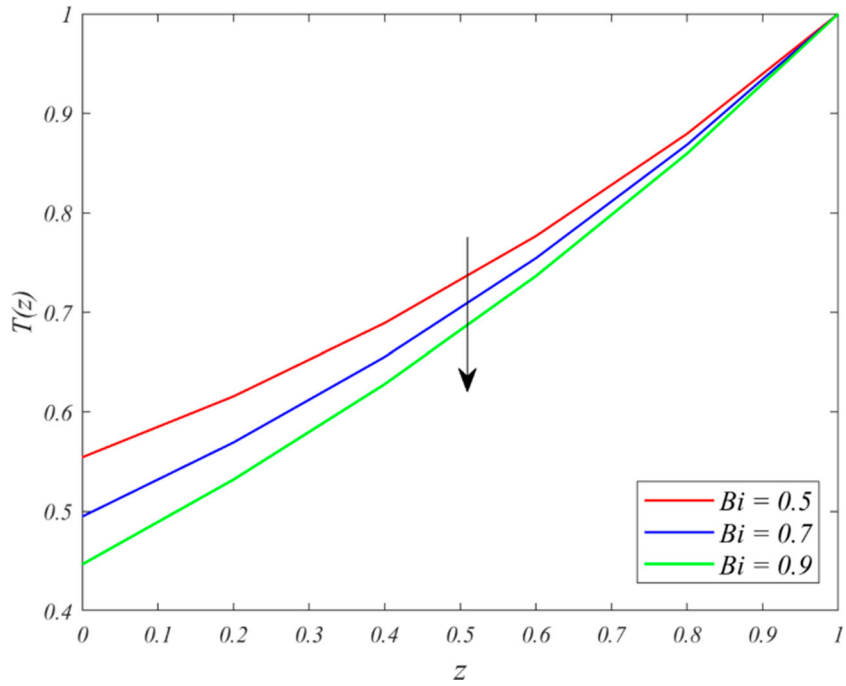


**Figure 14.** Effect of Bi in T.

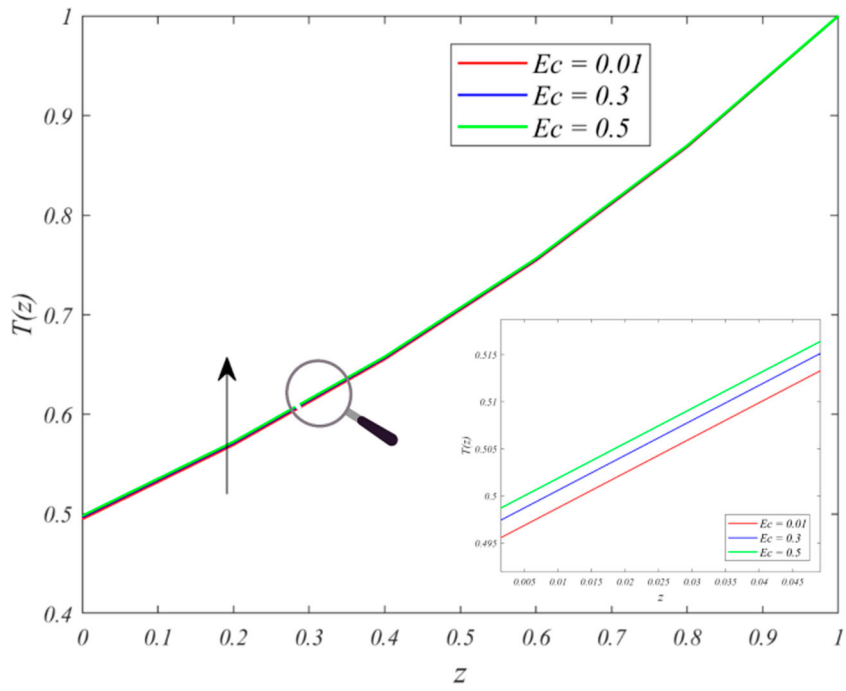


**Figure 15.** Effect of Ec in T.

The computed results obtained are compared with those reported by Kumar (2021). Table 3 shows a comparison with that of Kumar (2021) and is found in decent agreement.

## 6. Conclusion

- The velocity profiles are nearly parabolic in nature, having a maximum value close to the centreline of the channel
- The Casson parameter and the radiation parameter have an accelerating effect on the fluid velocity. But, the chemical reaction parameter, the heat sink parameter, and the Schmidt number have a decelerating effect on the fluid velocity.
- The impact of the Casson parameter and thermal Grashof number enhances the IMF on the first half of the midline of the channel, while an opposite effect on the second half is observed.
- The impact of the chemical reaction parameter reduces the IMF on the first half of the centreline while an opposite effect on the second half is seen.

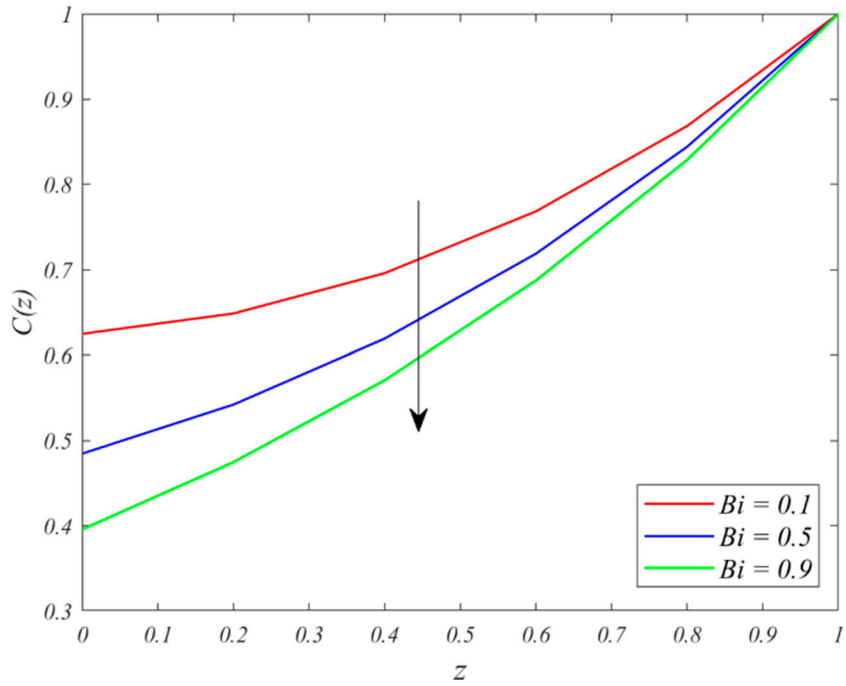


**Figure 16.** Effect of Bi in C.

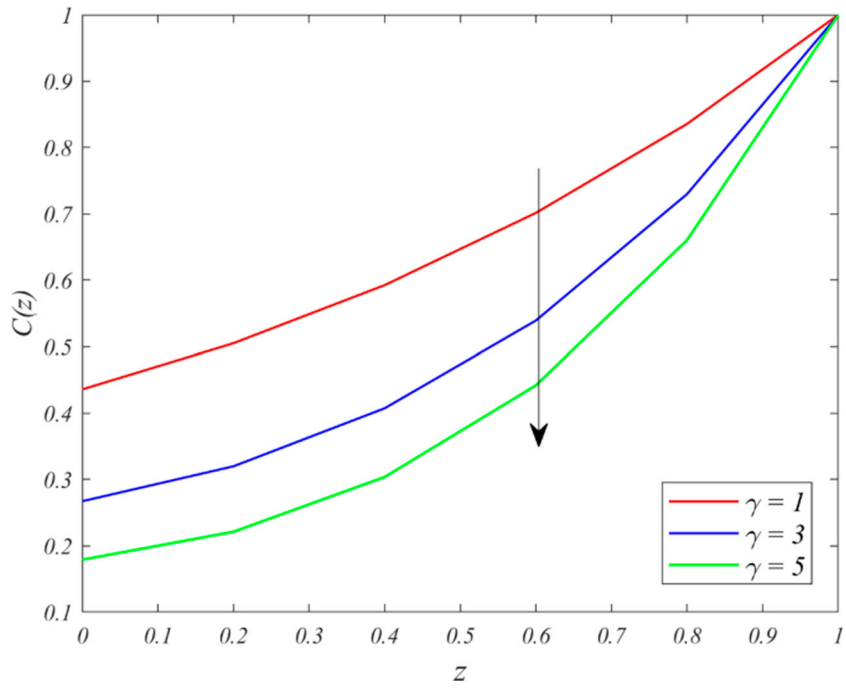


**Figure 17.** Effect of $\gamma$ in C.

- ICD in the centreline of the channel decreases due to influences of chemical reaction parameter and heat sink parameter, while it enhances due to Casson parameter.
- Temperature improves due to Eckert number. Heat sink parameter and thermal Biot number reduces the temperature of the fluid profile.
- Concentration reduces due to chemical reaction parameter, thermal Biot number and Schmidt number.
- Nusselt number enhances with Casson parameter, radiation parameter, and Eckert number at both the surfaces $z = 0$ and $z = 1$.
- Skin friction enhances with the Casson parameter, radiation parameter, and Eckert number at both the surfaces $z = 0$ and $z = 1$, while the chemical reaction parameter shows the opposite impact.

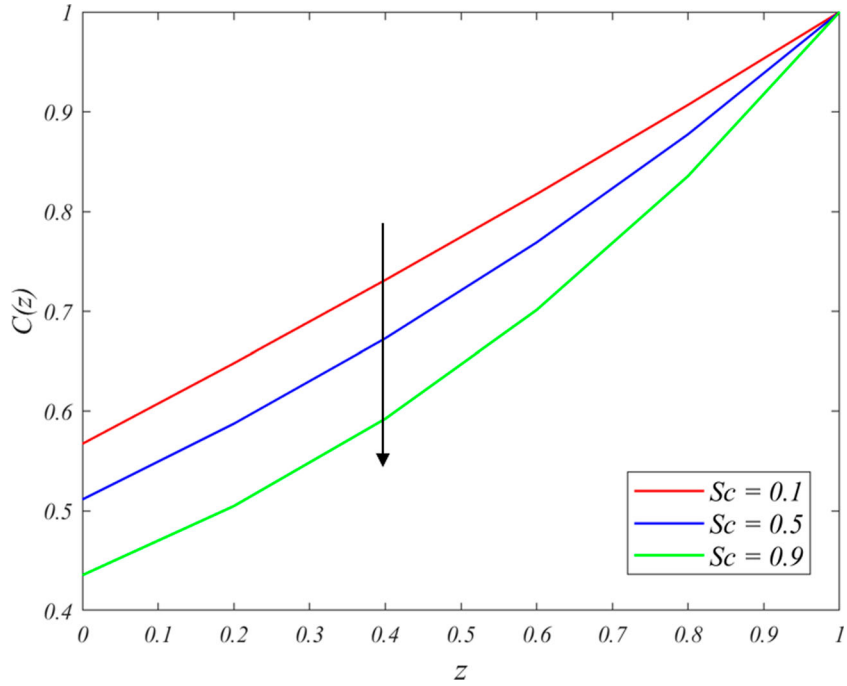


**Figure 18.** Effect of Sc in C.

**Table 1.** Nusselt Number Table for $Sc = 0.9$, $Ha = 5$, $S = 1$, $G = 1$, $G_1 = 1$, $Bi = -0.2$, $Pr = 0.63$, $\gamma = 1$.

| $\beta$ | Rd | $Ec$ | $\{Nu\}_{z=0}$ | $\{Nu\}_{z=1}$ |
|---|---|---|---|---|
| 1 | 1 | 0.01 | 0.191696 | −0.278160 |
| 2 | 1 | 0.01 | 0.191705 | −0.278071 |
| 3 | 1 | 0.01 | 0.191709 | −0.278029 |
| 1 | **1** | 0.01 | 0.191696 | −0.278160 |
| 1 | **2** | 0.01 | 0.208348 | −0.122556 |
| 1 | **4** | 0.01 | 0.223495 | 0.015359 |
| 1 | 1 | **0.01** | 0.191696 | −0.278160 |
| 1 | 1 | **0.3** | 0.192687 | −0.268683 |
| 1 | 1 | **0.5** | 0.193370 | −0.262148 |

**Table 2.** Numerical values for dimensionless skin frictions and mass flux for $Sc = 0.9$, $Ha = 5$, $S = 1$, $G = 1$, $G_1 = 1$, $Bi = 0.7$, $Pr = 0.63$.

| $\beta$ | $\gamma$ | $Rd$ | $Ec$ | $\tau_0$ | $\tau_1$ | $Q$ |
|---|---|---|---|---|---|---|
| 2 | 1 | 1 | 0.01 | 0.4151 | 0.5091 | 0.0610 |
| 3 | 1 | 1 | 0.01 | 0.4681 | 0.5716 | 0.0672 |
| 4 | 1 | 1 | 0.01 | 0.5000 | 0.6091 | 0.0707 |
| 2 | **1** | 1 | 0.01 | 0.4151 | 0.5091 | 0.0610 |
| 2 | **2** | 1 | 0.01 | 0.3827 | 0.4847 | 0.0569 |
| 2 | **3** | 1 | 0.01 | 0.3594 | 0.4667 | 0.0539 |
| 2 | 1 | **1** | 0.01 | 0.4151 | 0.5091 | 0.0610 |
| 2 | 1 | **2** | 0.01 | 0.4241 | 0.5157 | 0.0621 |
| 2 | 1 | **4** | 0.01 | 0.4318 | 0.5214 | 0.0630 |
| 2 | 1 | 1 | **0.01** | 0.4151 | 0.5091 | 0.0610 |
| 2 | 1 | 1 | **0.3** | 0.4156 | 0.5095 | 0.0611 |
| 2 | 1 | 1 | **0.5** | 0.4159 | 0.5097 | 0.0612 |

- Mass flux in the system enhances with the Casson parameter, radiation parameter, and Eckert number, whereas chemical reaction parameter shows reverse trend.

This type of study will be useful for biomedical engineering and many types of medical treatments, particularly the thermal therapeutic procedure. For the design of the relevant equipment, the thermal radiation heat transfer is crucial. Bursitis can also be treated with it.

**Table 3.** Comparison of skin-frictions (Taking Ha = 3).

| | | $\tau_0$ | | $\tau_1$ | |
|---|---|---|---|---|---|
| Bi | Rd | Kumar (2021) | Present result | Kumar (2021) | Present result |
| −0.1 | 1 | 0.438910 | 0.438909 | 0.458035 | 0.458035 |
| −0.1 | 2 | 0.467083 | 0.467082 | 0.476039 | 0.476039 |
| 1 | 1 | 0.300842 | 0.300842 | 0.383984 | 0.383983 |
| 1 | 2 | 0.312444 | 0.312443 | 0.392515 | 0.392514 |
| 2 | 1 | 0.258703 | 0.258703 | 0.361383 | 0.361382 |
| 2 | 2 | 0.266828 | 0.266828 | 0.367876 | 0.367876 |

## Disclosure statement

No potential conflict of interest was reported by the author(s).

## ORCID

*Utpal Jyoti Das* http://orcid.org/0000-0002-5482-5468
*Nayan Mani Majumdar* http://orcid.org/0000-0002-9590-068X

## References

Abdullahi, Faruk, Ibrahim Haliru Wala, and Muhammad Abdurrahman Sani. 2020. "Casson Fluid Flow Effects on MHD Unsteady Heat and Mass Transfer Free Convective Past an Infinite Vertical Plate." *International Journal of Scientific and Research Publications (IJSRP)* 10 (11): 104–118. doi:10.29322/ijsrp.10.11.2020.p10712.

Anantha Kumar, K., A. C. Venkata Ramudu, V. Sugunamma, and N. Sandeep. 2022. "Effect of Non-Linear Thermal Radiation on MHD Casson Fluid Flow Past a Stretching Surface with Chemical Reaction." *International Journal of Ambient Energy* 43 (1): 8400–8407. doi:10.1080/01430750.2022.2097947.

Arora, K. L. 1972. "Magnetohydrodynamic Flow Between Two Rotating Coaxial Cylinders Under Radial Magnetic Field." *The Physics of Fluids* 15 (6): 1146. doi:10.1063/1.1694041.

Arthur, Emmanuel Maurice, Ibrahim Yakubu Seini, and Letis Bortey Bortteir. 2015. "Analysis of Casson Fluid Flow Over a Vertical Porous Surface with Chemical Reaction in the Presence of Magnetic Field." *Journal of Applied Mathematics and Physics* 03 (06): 713–723. doi:10.4236/jamp.2015.36085.

Asogwa, K. K., and A. A. Ibe. 2020. ""A Study of MHD Casson Fluid Flow Over a Permeable Stretching Sheet with Heat and Mass Transfer." *Journal of Engineering Research and Reports*, 10–25. doi:10.9734/jerr/2020/v16i217161.

Basu, T., and D. N. Roy. 1985. "Laminar Heat Transfer in a Tube with Viscous Dissipation." *International Journal of Heat and Mass Transfer* 28 (3): 699–701. doi:10.1016/0017-9310(85)90191-7.

Brinkman, H. C. 1951. "Heat Effects in Capillary Flow I." *Applied Scientific Research* 2 (1): 120–124. doi:10.1007/bf00411976.

Casson, N. 1959. *A Flow Equation for Pigment-Oil Suspensions of the Printing Ink Type. Reprinted from "Rheology of Disperse Systems"*. Oxford: Pergamon Press.

Cramer, Kenneth R. 1973. "New from Mcgraw-Hill Magnetofluid Dynamics for Engineers and Applied Physicists." *Electrical Engineering in Japan* 93 (1): 142–142. doi:10.1002/eej.4390930120.

Daniel, Yahaya Shagaiya, Zainal Abdul Aziz, Zuhaila Ismail, and Faisal Salah. 2018. "Impact of Thermal Radiation on Electrical MHD Flow of Nanofluid Over Nonlinear Stretching Sheet with Variable Thickness." *Alexandria Engineering Journal* 57 (3): 2187–2197. doi:10.1016/j.aej.2017.07.007.

Das, Utpal Jyoti. 2021. "An Unsteady MHD Flow of Casson Fluid Past an Exponentially Accelerated Vertical Plate." *Latin American Applied Research - An International Journal* 51 (4): 309–314. doi:10.52292/j.laar.2021.588.

Elbashbeshy, Elsayed, and T. G. Emam. 2011. "Effects of Thermal Radiation and Heat Transfer Over an Unsteady Stretching Surface Embedded in a Porous Medium in the Presence of Heat Source or Sink." *Thermal Science* 15 (2): 477–485. doi:10.2298/tsci1102477e.

Globe, Samuel. 1959. "Laminar Steady-State Magnetohydrodynamic Flow in an Annular Channel." *Physics of Fluids* 2 (4): 404. doi:10.1063/1.1724410.

Gokulavani, P., M. Muthtamilselvan, and Qasem Al-Mdallal. 2022. ""Double Diffusive Convection of CuO+MWCNT Hybrid Nanofluid in an Inclined Open Cavity with Internal Heat Generation/Absorption." *International Journal of Ambient Energy*, 1–11. doi:10.1080/01430750.2022.2128417.

Gregory, Thomas Stanley, Rui Cheng, Guoyi Tang, Leidong Mao, and Zion Tsz Ho Tse. 2016. "The Magnetohydrodynamic Effect and Its Associated Material Designs for Biomedical Applications: A State-of-the-art Review." *Advanced Functional Materials* 26 (22): 3942–3952. doi:10.1002/adfm.201504198.

Guria, M., B. K. Das, R. N. Jana, and S. K. Ghosh. 2007. "Effects of Wall Conductance on MHD Fully Developed Flow with Asymmetric Heating of the Wall." *Fluid Mechanics Research* 34 (6): 521–534. doi:10.1615/interjfluidmechres.v34.i6.40.

Hamza, M. M., I. G. Usman, and A. Sule. 2015. "Unsteady/Steady Hydromagnetic Convective Flow Between Two Vertical Walls in the Presence of Variable Thermal Conductivity." *Journal of Fluids* 2015: 1–9. doi:10.1155/2015/358053.

Hari Krishna, Y., Gurrampati Venkata Ramana Reddy, and Oluwole Daniel Makinde. 2018. "Chemical Reaction Effect on MHD Flow of Casson Fluid with Porous Stretching Sheet." *Defect and Diffusion Forum* 389: 100–109. doi:10.4028/www.scientific.net/ddf.389.100.

Hassan, Ali, Azad Hussain, Mubashar Arshad, Soumaya Gouadria, Jan Awrejcewicz, Ahmed M. Galal, Fahad M. Alharbi, and S. Eswaramoorthi. 2022. "Insight Into the Significance of Viscous Dissipation and Heat Generation/Absorption in Magneto-Hydrodynamic Radiative Casson Fluid Flow with First-Order Chemical Reaction." *Frontiers in Physics* 10 (August), doi:10.3389/fphy.2022.920372.

Hussain, Shafqat, Noura Alsedias, and Abdelraheem M. Aly. 2022. "Natural Convection of a Water-Based Suspension Containing Nano-Encapsulated Phase Change Material in a Porous Grooved Cavity." *Journal of Energy Storage* 51 (July): 104589. doi:10.1016/j.est.2022.104589.

Hussain, Shafqat, Abdelraheem M. Aly, and Noura Alsedias. 2022. "Bioconvection of Oxytactic Microorganisms with Nano-Encapsulated Phase Change Materials in an Omega-Shaped Porous Enclosure." *Journal of Energy Storage* 56 (December): 105872. doi:10.1016/j.est.2022.105872.

Hussain, Shafqat, Abdelraheem M. Aly, and Hakan F. Öztop. 2022. "Magneto-Bioconvection Flow of Hybrid Nanofluid in the Presence of Oxytactic Bacteria in a Lid-Driven Cavity with a Streamlined Obstacle." *International Communications in Heat and Mass Transfer* 134 (May): 106029. doi:10.1016/j.icheatmasstransfer.2022.106029.

Hussain, Shafqat, Muhammad Jamal, Zoubida Haddad, and Müslüm Arıcı. 2022. "Numerical Modeling of Magnetohydrodynamic Thermosolutal Free Convection of Power Law Fluids in a Staggered Porous Enclosure." *Sustainable Energy Technologies and Assessments* 53 (October): 102395. doi:10.1016/j.seta.2022.102395.

Hussain, Shafqat, Zehba Raizah, and Abdelraheem M. Aly. 2022. "Thermal Radiation Impact on Bioconvection Flow of Nano-Enhanced Phase Change Materials and Oxytactic Microorganisms Inside a Vertical Wavy Porous Cavity." *International Communications in Heat and Mass Transfer* 139 (December): 106454. doi:10.1016/j.icheatmasstransfer.2022.106454.

Hussain, Shafqat, Muhammad Zeeshan, and Dur-e-Shehwar Sagheer. 2022. "Irreversibility Analysis for the Natural Convection of Casson Fluid in an Inclined Porous Cavity Under the Effects of Magnetic Field and Viscous Dissipation." *International Journal of Thermal Sciences* 179 (September): 107699. doi:10.1016/j.ijthermalsci.2022.107699.

Jha, B. K., and B. Aina. 2017. "Effect of Induced Magnetic Field on MHD Mixed Convection Flow in Vertical Microchannel." *International Journal of Applied Mechanics and Engineering* 22 (3): 567–582. doi:10.1515/ijame-2017-0036.

Jha, Basant K., and Babatunde Aina. 2018. "Impact of Viscous Dissipation on Fully Developed Natural Convection Flow in a Vertical Microchannel." *Journal of Heat Transfer* 140 (9): 094502. doi:10.1115/1.4039641.

Jha, Basant K., and Clement A. Apere. 2011. "Magnetohydrodynamic Free Convective Couette Flow With Suction and Injection." *Journal of Heat Transfer* 133 (9), doi:10.1115/1.4003902.

Jha, B. K., and Sani Isa. 2013. "Computational Treatment of MHD Transient Natural Convection Flow in a Vertical Channel Due to Symmetric Heating in Presence of Induced Magnetic Field." *Journal of the Physical Society of Japan* 82 (8): 084401. doi:10.7566/jpsj.82.084401.

Kho, Y. B., A. Hussanan, M. K. A. Mohamed, N. M. Sarif, Z. Ismail, and M. Z. Salleh. 2017. "Thermal Radiation Effect on MHD Flow and Heat Transfer Analysis of Williamson Nanofluid Past Over a Stretching Sheet with Constant Wall Temperature." *Journal of Physics. Conference Series* 890: 012034. doi:10.1088/1742-6596/890/1/012034.

Krishna, M. Veera, Kamboji Jyothi, and Ali J. Chamkha. 2020. "Heat and Mass Transfer on Mhd Flow of Second-Grade Fluid Through Porous Medium Over a Semi-Infinite Vertical Stretching Sheet." *Journal of Porous Media* 23 (8): 751–765. doi:10.1615/jpormedia.2020023817.

Kumar, Dileep. 2021. "Radiation Effect on Magnetohydrodynamic Flow with Induced Magnetic Field and Newtonian Heating/Cooling: An Analytic Approach." *Propulsion and Power Research* 10 (3): 303–313. doi:10.1016/j.jppr.2021.07.001.

Kumar, M. Anil, Y. Dharmendar Reddy, V. Srinivasa Rao, and B. Shankar Goud. 2021. "Thermal Radiation Impact on MHD Heat Transfer Natural Convective Nano Fluid Flow Over an Impulsively Started Vertical Plate." *Case Studies in Thermal Engineering* 24 (100826): 100826. doi:10.1016/j.csite.2020.100826.

Kumar, Dileep, A. K. Singh, and Devendra Kumar. 2020. "Influence of Heat Source/Sink on MHD Flow Between Vertical Alternate Conducting Walls with Hall Effect." *Physica A: Statistical Mechanics and its Applications* 544 (123562): 123562. doi:10.1016/j.physa.2019.123562.

Loh, A. K. W., G. M. Chen, and B. K. Lim. 2022. "Viscous Dissipation Effect on Forced Convective Transport of Nanofluids in an Asymmetrically Heated Parallel-Plate Microchannel." *Case Studies in Thermal Engineering* 35 (102056): 102056. doi:10.1016/j.csite.2022.102056.

Mohamad, Ahmad Qushairi, Nurul Aini Jaafar, Sharidan Shafie, Zulkhibri Ismail, and Muhammad Qasim. 2019. "Theoretical Study on Rotating Casson Fluid in Moving Channel Disk." *Journal of Physics: Conference Series* 1366 (1): 012039. doi:10.1088/1742-6596/1366/1/012039.

Mukhopadhyay, Swati, Prativa Ranjan De, Krishnendu Bhattacharyya, and G. C. Layek. 2013. "Casson Fluid Flow Over an Unsteady Stretching Surface." *Ain Shams Engineering Journal* 4 (4): 933–938. doi:10.1016/j.asej.2013.04.004.

Naseem, Tahir, Urooj Fatima, Mohammad Munir, Azeem Shahzad, Nasreen Kausar, Kottakkaran Sooppy Nisar, C. Ahamed Saleel, and Mohamed

Abbas. 2022. "Joule Heating and Viscous Dissipation Effects in Hydromagnetized Boundary Layer Flow with Variable Temperature." *Case Studies in Thermal Engineering* 35 (102083): 102083. doi:10.1016/j.csite.2022.102083.

Nayak, B., S. Acharya, and S. R. Mishra. 2022. "Impact of Dissipative Heat and Thermal Radiation on the Steady Magnetohydrodynamic Nanofluid Flow with an Interaction of Brownian Motion and Chemical Reaction." *International Journal of Applied and Computational Mathematics* 8: 3. doi:10.1007/s40819-022-01345-x.

Prakash, D., E. Ragupathi, M. Muthtamilselvan, Bahaaeldin Abdalla, and Qasem M. Al Mdallal. 2021. "Impact of Boundary Conditions of Third Kind on Nanoliquid Flow and Radiative Heat Transfer Through Asymmetrical Channel." Case Studies in Thermal Engineering 28 (December). 101488. doi:10.1016/j.csite.2021.101488.

Pramanik, S. 2014. "Casson Fluid Flow and Heat Transfer Past an Exponentially Porous Stretching Surface in Presence of Thermal Radiation." *Ain Shams Engineering Journal* 5 (1): 205–212. doi:10.1016/j.asej.2013.05.003.

Ramudu, Venkata, A. C. K, Anantha Kumar, V. Sugunamma, and N. Sandeep. 2021. "Impact of Soret and Dufour on MHD Casson Fluid Flow Past a Stretching Surface with Convective–Diffusive Conditions." *Journal of Thermal Analysis and Calorimetry* 147 (3): 2653–2663. doi:10.1007/s10973-021-10569-w.

Rashidi, Saman, Javad Abolfazli Esfahani, and Mahla Maskaniyan. 2017. "Applications of Magnetohydrodynamics in Biological Systems-a Review on the Numerical Studies." *Journal of Magnetism and Magnetic Materials* 439: 358–372. doi:10.1016/j.jmmm.2017.05.014.

Reddy, Minnam, Vasudeva Reddy, A. Sreevallabha Reddy, R. Suresh Babu, and N. Sandeep. 2022. "Effect of Nanospray on Hydrodynamic Cylindrical Film Flow of Sutterby–Casson Nanoliquids: A Renewable Energy Application." *Proceedings of the Institution of Mechanical Engineers, Part E: Journal of Process Mechanical Engineering*, 095440892211059. doi:10.1177/09544089221105938

Sandeep, N., C. Sulochana, and G. P. Ashwinkumar. 2022. "Understanding the Dynamics of Chemically Reactive Casson Liquid Flow Above a Convectively Heated Curved Expanse." *Proceedings of the Institution of Mechanical Engineers, Part C: Journal of Mechanical Engineering Science* 236 (24): 11420–11430. doi:10.1177/09544062221115084.

Saranya, S., Qasem M. Al-Mdallal, and I. L. Animasaun. 2022. "Shifted Legendre Collocation Analysis of Time-Dependent Casson Fluids and Carreau Fluids Conveying Tiny Particles and Gyrotactic Microorganisms: Dynamics on Static and Moving Surfaces." *Arabian Journal for Science and Engineering*, doi:10.1007/s13369-022-07087-8.

Sarveshanand, and A. K.Singh. 2015. "Magnetohydrodynamic Free Convection Between Vertical Parallel Porous Plates in the Presence of Induced Magnetic Field." *SpringerPlus* 4 (1): 333. doi:10.1186/s40064-015-1097-1.

Sedki, Ahmed M., S. M. Abo-Dahab, J. Bouslimi, and K. H. Mahmoud. 2021. "Thermal Radiation Effect on Unsteady Mixed Convection Boundary Layer Flow and Heat Transfer of Nanofluid Over Permeable Stretching Surface Through Porous Medium in the Presence of Heat Generation." *Science Progress* 104 (3): 368504211042261. doi:10.1177/00368504211042261.

Shah, Nehad Ali, Hussam Alrabaiah, Dumitru Vieru, and Se-Jin Yook. 2022. "Induced Magnetic Field and Viscous Dissipation on Flows of Two Immiscible Fluids in a Rectangular Channel." *Scientific Reports* 12 (1): 39. doi:10.1038/s41598-021-03313-9.

Sharma, Bishwa R., Rita Choudhury, and Utpal J. Das. 2022. "Soret–Dufour Effects on Chemically Reacting Non-Darcian MHD Flow Around a Plate." *Heat Transfer*, 52(1), 28–39. doi:10.1002/htj.22684.

Shateyi, Stanford, and Sandile Sydney Motsa. 2009. "Thermal Radiation Effects on Heat and Mass Transfer Over an Unsteady Stretching Surface." *Mathematical Problems in Engineering* 2009: 1–13. doi:10.1155/2009/965603.

Sheikholeslami, M., M. M. Rashidi, T. Hayat, and D. D. Ganji. 2016. "Free Convection of Magnetic Nanofluid Considering MFD Viscosity Effect." *Journal of Molecular Liquids* 218: 393–399. doi:10.1016/j.molliq.2016.02.093.

Singh, R. K., and A. K. Singh. 2012. "Effect of Induced Magnetic Field on Natural Convection in Vertical Concentric Annuli." *Li Xue Xue Bao [Acta Mechanica Sinica]* 28 (2): 315–323. doi:10.1007/s10409-012-0052-4.

Singh, Rajiv K., Ashok K. Singh, Nirmal C. Sacheti, and Pallath Chandran. 2010. "On Hydromagnetic Free Convection in the Presence of Induced Magnetic Field." *Warme- Und Stoffubertragung [Heat and Mass Transfer]* 46 (5): 523–529. doi:10.1007/s00231-010-0594-6.

Vijayalakshmi, R., and A. Govindarajan. 2019. "Impact of Heat Transfer and Viscous Dissipation on Unsteady MHD Oscillatory Dusty Fluid Flow Through a Vertical Porous Channel." *Journal of Physics. Conference Series* 1377 (1): 012025. doi:10.1088/1742-6596/1377/1/012025.

Vishnu Ganesh, N., Qasem M. Al-Mdallal, G. Hirankumar, R. Kalaivanan, and Ali J. Chamkha. 2022b. "Buoyancy-Driven Convection of MWCNT – Casson Nanofluid in a Wavy Enclosure with a Circular Barrier and Parallel Hot/Cold Fins." *Alexandria Engineering Journal* 61 (4): 3249–3264. doi:10.1016/j.aej.2021.08.055.

Vishnu Ganesh, N., Qasem M. Al-Mdallal, Hakan F. Öztop, and R. Kalaivanan. 2022a. "Analysis of Natural Convection for a Casson-Based Multiwall Carbon Nanotube Nanofluid in a Partially Heated Wavy Enclosure with a Circular Obstacle in the Presence of Thermal Radiation." *Journal of Advanced Research* 39 (July): 167–185. doi:10.1016/j.jare.2021.10.006.

## APPENDIX

$$m_1 = \sqrt{Sc\lambda}, \quad N = \sqrt{S/(1+Rd)}, \quad B = 1 + \frac{1}{\beta}, \quad K = \frac{Ha}{\sqrt{B}}, \quad K_1 = -PrB/(1+Rd),$$

$$K_2 = -Ha^2 Pr/(1+Rd), \quad A_1 = \frac{m_1 + Bi}{(m_1+Bi)e^{m_1} + (m_1 - Bi)e^{-m_1}}, \quad A_2 = \frac{m_1 - Bi}{(m_1+Bi)e^{m_1} + (m_1 - Bi)e^{-m_1}},$$

$$A_3 = \frac{N+Bi}{(N+Bi)e^{N} + (N-Bi)e^{-N}}, \quad A_4 = \frac{N-Bi}{(N+Bi)e^{N} + (N-Bi)e^{-N}}, \quad A_8 = \frac{G}{BN(N^2-K^2)},$$

$$A_9 = \frac{G_1}{Bm_1(m_1^2-K^2)}, \quad A_{10} = A_8A_3, A_{11} = A_8A_4, \quad A_{12} = A_9A_1, \quad A_{12} = A_9A_1, \quad A_{13} = A_9A_2,$$

$$A_6 = \frac{-A_{10}(e^N-1)(N+K) - A_{11}(e^{-N}-1)(N-K) - A_{12}(e^{m1}-1)(m_1+K) - A_{13}(e^{-m1}-1)(m_1-K)}{2K(e^K-1)};$$

$$A_7 = \frac{A_{10}(e^N-1)(N-K) + A_{11}(e^{-N}-1)(N+K) + A_{12}(e^{m1}-1)(m_1-K) + A_{13}(e^{-m1}-1)(m_1+K)}{2K(e^{-K}-1)};$$

$$A_5 = -(A_6 + A_7 + A_{10}) + A_{11} - A_{12} + A_{13}; \quad A_{14} = A_6K - A_7K + A_{10}N + A_{11}N + A_{12}m_1 + A_{13}m_1$$

$$A_{17} = A_7^2K^4K_1, \quad A_{18} = A_6^2K^4K_1, \quad A_{19} = A_{10}^2N^4K_1, \quad A_{20} = A_{11}^2N^4K_1, \quad A_{21} = A_{12}^2m_1^4K_1, \quad A_{22} = A_{13}^2m_1^4K_1,$$

$$A_{23} = 2(A_6A_7K^4 - A_{10}A_{11}N^4 - A_{12}A_{13}m_1^4)K_1, \quad A_{24} = 2A_6A_{10}K^2N^2K_1, \quad A_{25} = 2A_6A_{11}K^2N^2K_1,$$

$$A_{26} = 2A_6A_{12}K^2m_1^2K_1, \quad A_{27} = 2A_6A_{13}K^2m_1^2K_1, \quad A_{28} = 2A_7A_{10}K^2N^2K_1, \quad A_{29} = 2A_7A_{11}K^2N^2K_1,$$

$$A_{30} = 2A_7A_{12}K^2m_1^2K_1, \quad A_{31} = 2A_7A_{13}K^2m_1^2K_1, \quad A_{32} = 2A_{10}A_{12}N^2m_1^2K_1, \quad A_{33} = 2A_{10}A_{13}N^2m_1^2K_1,$$

$$A_{34} = 2A_{11}A_{12}N^2m_1^2K_1, \quad A_{35} = 2A_{11}A_{13}N^2m_1^2K_1, \quad A_{36} = A_6^2K^2K_2, \quad A_{37} = A_7^2K^2K_2, \quad A_{38} = A_{10}^2N^2K_2,$$

$$A_{39} = A_{11}^2N^2K_2, \quad A_{40} = A_{12}^2m_1^2K_2, \quad A_{41} = A_{13}^2m_1^2K_2, \quad A_{42} = -2(A_6A_7K^2 - A_{10}A_{11}N^2 - A_{12}A_{13}m_1^2)K_2,$$

$$A_{43} = 2A_6A_{10}KNK_2, \quad A_{44} = 2A_6A_{11}KNK_2, \quad A_{45} = 2A_6A_{12}Km_1K_2, \quad A_{46} = 2A_6A_{13}Km_1K_2,$$

$$A_{47} = 2A_7A_{10}KNK_2, \quad A_{48} = 2A_7A_{11}KNK_2, \quad A_{49} = 2A_7A_{12}Km_1K_2, \quad A_{50} = 2A_7A_{13}Km_1K_2,$$

$$A_{51} = 2A_{10}A_{12}Nm_1K_2, \quad A_{52} = 2A_{10}A_{13}Nm_1K_2, \quad A_{53} = 2A_{11}A_{12}Nm_1K_2, \quad A_{54} = 2A_{11}A_{13}Nm_1K_2,$$

$$A_{55} = A_{17} + A_{36}, \quad A_{56} = A_{18} + A_{37}, \quad A_{57} = A_{19} + A_{38}, \quad A_{58} = A_{20} + A_{39}, \quad A_{59} = A_{21} + A_{40},$$

$$A_{60} = A_{22} + A_{41}, \quad A_{61} = A_{23} + A_{42}, \quad A_{62} = A_{24} + A_{43}, \quad A_{63} = A_{44} - A_{25}, \quad A_{64} = A_{26} + A_{45},$$

$$A_{65} = A_{46} - A_{27}, \quad A_{66} = A_{28} - A_{47}, \quad A_{67} = -A_{29} - A_{48}, \quad A_{68} = A_{30} - A_{49}, \quad A_{69} = -A_{31} - A_{50},$$

$$A_{70} = A_{32} + A_{51}, \quad A_{71} = A_{52} - A_{33}, \quad A_{72} = A_{53} - A_{34}, \quad A_{73} = A_{35} + A_{54}, \quad A_{74} = \frac{A_{55}}{4K^2 - N^2},$$

$$A_{75} = \frac{A_{56}}{4K^2 - N^2}, \quad A_{76} = \frac{A_{57}}{3N^2}, \quad A_{77} = \frac{A_{58}}{3N^2}, \quad A_{78} = \frac{A_{59}}{4m_1^2 - N^2}, \quad A_{79} = \frac{A_{60}}{4m_1^2 - N^2}, \quad A_{80} = \frac{A_{61}}{-N^2},$$

$$A_{81} = \frac{A_{62}}{(K+N)^2 - N^2}, \quad A_{82} = \frac{A_{67}}{(K+N)^2 - N^2}, \quad A_{83} = \frac{A_{63}}{(K-N)^2 - N^2}, \quad A_{84} = \frac{A_{66}}{(K-N)^2 - N^2},$$

$$A_{85} = \frac{A_{64}}{(K+m_1)^2 - N^2}, \quad A_{86} = \frac{A_{69}}{(K+m_1)^2 - N^2}, \quad A_{87} = \frac{A_{65}}{(K-m_1)^2 - N^2}, \quad A_{88} = \frac{A_{68}}{(K-m_1)^2 - N^2},$$

$$A_{89} = \frac{A_{70}}{(N+m_1)^2 - N^2}, \quad A_{90} = \frac{A_{73}}{(N+m_1)^2 - N^2}, \quad A_{91} = \frac{A_{71}}{(N-m_1)^2 - N^2}, \quad A_{92} = \frac{A_{72}}{(N-m_1)^2 - N^2},$$

$$P_1 = 2A_{74}K - 2A_{75}K + 2NA_{76} - 2A_{77}N + 2m_1A_{78} - 2m_1A_{79} + (K+N)A_{81} - (K+N)A_{82} + (K-N)A_{83} - (K-N)A_{84} + (K+m1)A_{85}$$
$$- (K+m1)A_{86} + (K-m1)A_{87} - (K-m1)A_{88} + (N+m1)A_{89} - (N+m1)A_{90} + (N-m1)A_{91} - (N-m1)A_{92},$$

$$P_2 = A_{74} + A_{75} + A_{76} + A_{77} + A_{78} + A_{79} + A_{80} + A_{81} + A_{82} + A_{83} + A_{84} + A_{85} + A_{86} + A_{87} + A_{88} + A_{89} + A_{90} + A_{91} + A_{92},$$

$$P_3 = -[A_{74}e^{2K} + A_{75}e^{-2K} + A_{76}e^{2N} + A_{77}e^{-2N} + A_{78}e^{2m_1} + A_{79}e^{-2m_1} + A_{80} + A_{81}e^{K+N} + A_{82}e^{-(K+N)} + A_{83}e^{(K-N)} + A_{84}e^{-(K-N)} + A_{85}e^{(K+m1)}$$
$$+ A_{86}e^{-(K+m1)} + A_{87}e^{(K-m1)} + A_{88}e^{-(K-m1)} + A_{89}e^{(N+m1)} + A_{90}e^{-(N+m1)} + A_{91}e^{(N-m1)} + A_{92}e^{-(N-m1)}],$$

$$A_{15} = \frac{-P_1 + P_2Bi + (N+Bi)e^NP_3}{(N-Bi) + (N+Bi)e^{2N}}, \quad A_{16} = P_3e^N - A_{15}e^{2N}, \quad A_{96} = \frac{G}{B}\frac{A_{15}}{N(N^2-K^2)},$$

$$A_{97} = \frac{G}{B}\frac{A_{16}}{N(N^2-K^2)}, \quad A_{98} = \frac{G}{B}\frac{A_{74}}{6K^3}, \quad A_{99} = \frac{G}{B}\frac{A_{75}}{6K^3}, \quad A_{100} = \frac{G}{B}\frac{A_{76}}{2N(4N^2-K^2)},$$

$$A_{101} = \frac{G}{B}\frac{A_{77}}{2N(4N^2-K^2)}, \quad A_{102} = \frac{G}{B}\frac{A_{78}}{2m_1(4m_1^2-K^2)}, \quad A_{103} = \frac{G}{B}\frac{A_{79}}{2m_1(4m_1^2-K^2)},$$

$$A_{104} = -\frac{G}{B}\frac{A_{80}}{K^2}, \quad A_{105} = \frac{G}{B}\frac{A_{81}}{(K+N)[2KN+N^2]}, \quad A_{106} = \frac{G}{B}\frac{A_{82}}{(K+N)[2KN+N^2]},$$

$$A_{107} = \frac{G}{B}\frac{A_{83}}{(K-N)[N^2-2KN]}, \quad A_{108} = \frac{G}{B}\frac{A_{84}}{(K-N)[N^2-2KN]}, \quad A_{109} = \frac{G}{B}\frac{A_{85}}{(K+m_1)[m_1^2+2Km_1]},$$

$$A_{110} = \frac{G}{B}\frac{A_{86}}{(K+m_1)[m_1^2+2Km_1]}, \quad A_{111} = \frac{G}{B}\frac{A_{87}}{(K-m_1)[m_1^2-2Km_1]}, \quad A_{112} = \frac{G}{B}\frac{A_{88}}{(K-m_1)[m_1^2-2Km_1]},$$

$$A_{113} = \frac{G}{B}\frac{A_{89}}{(N+m_1)[(N+m_1)^2-K^2]}, \quad A_{114} = \frac{G}{B}\frac{A_{90}}{(N+m_1)[(N+m_1)^2-K^2]},$$

$$A_{115} = \frac{G}{B}\frac{A_{91}}{(N-m_1)[(N-m_1)^2-K^2]}, \quad A_{116} = \frac{G}{B}\frac{A_{92}}{(N-m_1)[(N-m_1)^2-K^2]},$$

$$\begin{aligned}
P_5 = {} & -[A_{96}e^{N} - A_{97}e^{-N} + A_{98}e^{2K} - A_{99}e^{-2K} + A_{100}e^{2N} - A_{101}e^{-2N} + A_{102}e^{2m_1} - A_{103}e - 2m_1 \\
& + A_{104} + A_{105}e^{(K+N)} - A_{106}e^{-(K+N)} + A_{107}e^{(K-N)} - A_{108}e^{-(K-N)} + A_{109}e^{(K+m_1)} - A_{110}e^{-(K+m_1)} \\
& + A_{111}e^{(K-m_1)} - A_{112}e^{-(K-m_1)} + A_{113}e^{(N+m_1)} - A_{114}e^{-(N+m_1)} + A_{115}e^{(N-m_1)} - A_{116}e^{-(N-m1)}], \\
P_6 = {} & N(A_{96}+A_{97}) + 2K(A_{98}+A_{99}) + 2N(A_{100}+A_{101}) + 2m_1(A_{102}+A_{103}) + (K+N)(A_{105}+A_{106}) \\
& + (K-N)(A_{107}+A_{108}) + (K+m_1)(A_{109}+A_{110}) + (K-m_1)(A_{111}+A_{112}) \\
& + (N+m_1)(A_{113}+A_{114}) + (N-m_1)(A_{115}+A_{116}), \\
P_7 = {} & N(A_{96}e^{N} + A_{97}e^{-N}) + 2K(A_{98}e^{2K} + A_{99}e^{-2K}) + 2N(A_{100}e^{2N} + A_{101}e^{-2*N}) \\
& + 2m_1(A_{102}e^{2m_1} + A_{103}e^{-2m_1}) + (K+N)(A_{105}e^{(K+N)} + A_{106}e^{-(K+N)}) + (K-N)(A_{107}e^{(K-N)} \\
& + A_{108}e^{-(K-N)}) + (K+m_1)(A_{109}e^{(K+m_1)} + A_{110}e^{-(K+m_1))}) + (K-m_1)(A_{111}e^{(K-m_1)} + A_{112}e^{-(K-m_1)}) \\
& + (N+m_1)(A_{113}e^{(N+m_1)} + A_{114}e^{-(N+m_1)}) + (N-m_1)(A_{115}e^{(N-m_1)} + A_{116}e^{-(N-m1)}),
\end{aligned}$$

$$A_{94} = \frac{(P_5-P_4) + (\frac{P_6-P_7}{k})}{2(e^{K}-1)}, \quad A_{95} = \frac{(P_5-P_4) - (\frac{P_6-P_7}{k})}{2(e^{-K}-1)}, \quad A_{93} = P_4 - A_{94} - A_{95},$$

$$A_{117} = P_6 + A_{94}K - A_{95}K + A_{104}$$